Conductance of a Freestanding Conjugated Molecular Wire

Torben Jasper-Tönnies,[1,*] Aran Garcia-Lekue,[2,3] Thomas Frederiksen,[2,3] Sandra Ulrich,[4] Rainer Herges,[4] and Richard Berndt[1]

[1]*Institut für Experimentelle und Angewandte Physik, Christian-Albrechts-Universität zu Kiel, 24098 Kiel, Germany*
[2]*Donostia International Physics Center, DIPC, Paseo Manuel de Lardizabal 4, E-20018 Donostia-San Sebastián, Spain*
[3]*IKERBASQUE, Basque Foundation for Science, E-48013 Bilbao, Spain*
[4]*Otto-Diels-Institut für Organische Chemie, Christian-Albrechts-Universität zu Kiel, 24098 Kiel, Germany*

(Received 7 April 2017; revised manuscript received 6 June 2017; published 7 August 2017)

A freestanding molecular wire is placed vertically on Au(111) using a platform molecule and contacted by a scanning tunneling microscope. Despite the simplicity of the single-molecule junction, its conductance G reproducibly varies in a complex manner with the electrode separation. Transport calculations show that G is controlled by a deformation of the molecule, a symmetry mismatch between the tip and molecule orbitals, and the breaking of a C ≡ C triple in favor of a Au—C—C bond. This tip-controlled reversible bond formation or rupture alters the electronic spectrum of the junction and the states accessible for transport, resulting in an order of magnitude variation of the conductance.

DOI: 10.1103/PhysRevLett.119.066801

To measure the electrical conductance of a molecule two contacts are required. In a scanning tunneling microscope (STM) a metal sample and the tip of the microscope serve this purpose. However, preparing a single, freestanding molecule on a metal surface is difficult because simple molecules tend to increase their adsorption energy by lying flat on the substrate. Recent experiments succeeded in contacting oligomers at one of their ends, retracting the tip, and forming a partially freestanding wire [1–7]. Changes of the conductance during the pulling process have been attributed to the breaking of bonds to the substrate. Owing to the complexity of the investigated structure, significant variations occurred in repeated experiments. Related results along with the observation of a Kondo effect and molecular switching were reported for single perylene-tetracarboxylicacid-dianhydride or diarylethene molecules pulled off from a Ag or Au substrate [8–10]. A molecular bridge between two contacts may also be obtained by exposing a metallic junction to molecules that contain two reactive anchor groups and pulling the junction apart. With a certain probability, the desired geometry may occur in repeated experiments. This technique has been successfully used for several molecules but usually leads to scatter of the data because there is little control of the geometries of the investigated junctions [11,12].

We have solved the above-mentioned problems using a chemical approach and verified its success via STM imaging. We synthesized a molecule that is composed of a short propynyl moiety and an extended platform that lies flat on the substrate [13]. The propynyl wire is attached perpendicularly to the platform and stands upright on the surface. Related platform approaches involving different chemistry have been used to arrange molecular subunits parallel to a substrate or as an inclined cantilever (see, e.g., Refs. [14,15]). Moreover, rather than studying the rupture of a preformed contact, a contact is controllably made by moving the tip closer to the wire, starting from a nm distance until contact occurs. This process is fully reproducible, exhibits no hysteresis, and little scatter between different experimental runs on different molecules.

Despite the simplicity of our setup, we observe the conductance to vary in a complex manner. Using atomistic transport calculations we find that the tip initially causes the propynyl wire to bend. This hardly affects the electronic states of the molecule, but the match between the symmetries of the current-carrying states of the molecule and the tip worsens, and the conductance consequently is reduced. Upon further approach, the Au atom at the tip apex breaks the triple bond of propynyl and binds to the adjacent C atoms. This leads to new tip-molecule states accessible for transport, because unoccupied molecular orbitals strongly hybridize with tip states. As a result the conductance is enhanced and dominated by unoccupied instead of occupied molecular states.

Measurements were performed with a STM operated at 4.5 K and in ultrahigh vacuum (base pressure 10^{-9} Pa). Au(111) surfaces and chemically etched W tips were cleaned by repeated Ar^+ bombardment and annealing. After mounting into the STM the tips were repeatedly indented into the substrate. Finally, to ensure atomically sharp tips the sample was softly contacted until single Au atoms were deposited and the contacts were stable at conductance of $G \approx 1\ G_0 \doteq 2e^2/h$ (G_0: quantum of conductance, e: elementary charge, h: Planck constant). This indicates that the tip apex is comprised of a single Au atom. As a result, the contacted molecules are essentially probed by an s wave. We verified that tips were not modified during measurements on molecules by contacting

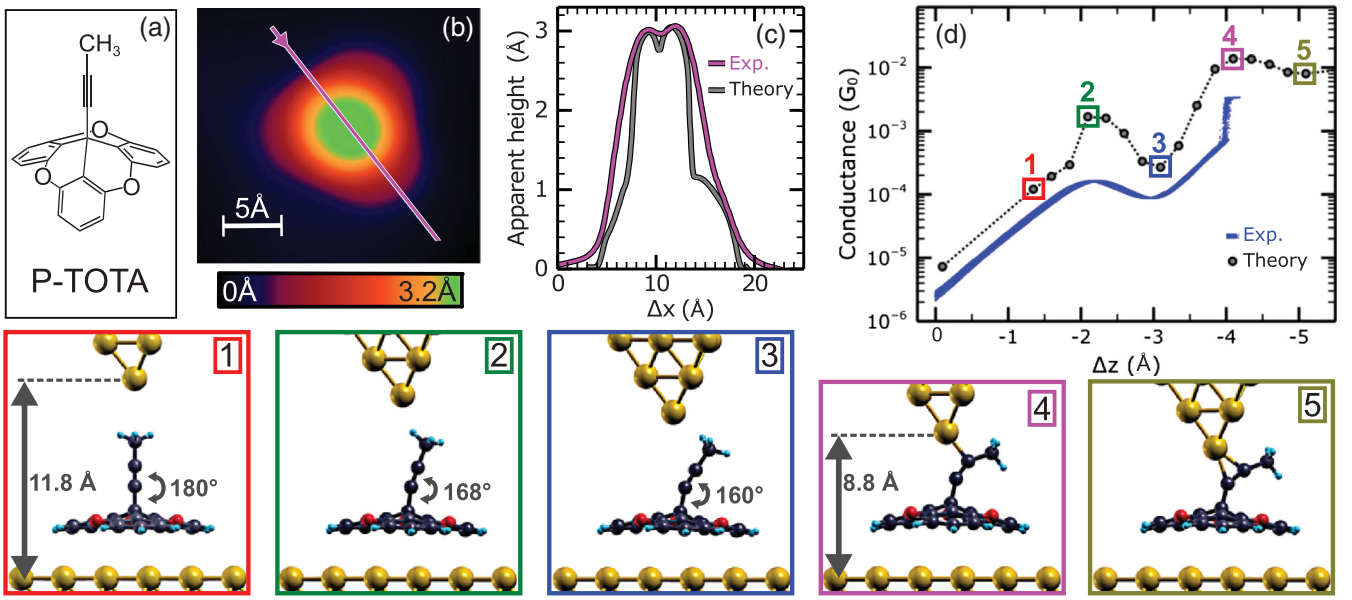

FIG. 1. (a) Lewis structure of propynyl-trioxatriangulenium (P-TOTA). (b) Constant-current STM topograph of a single P-TOTA ($V = 100$ mV, $I = 30$ pA). (c) Experimental apparent height profile along the line indicated in (b) and the corresponding theoretical profile scaled by an arbitrary factor of 0.5 [16]. (d) Experimental and theoretical conductance curves $G(\Delta z)$ of P-TOTA. The experimental conductance curve consists of 40 forward and 40 backward traces. Zero tip displacement is defined for the experimental curve by feedback loop parameters of 19 pA and 100 mV, whereas for the theoretical data points it corresponds to a distance z of 13.1 Å between apex atom and Au surface. (**1**–**5**) Calculated junction geometries corresponding to $\Delta z = -1.3, -2.1, -3.1, -4.1, -5.1$ Å as indicated in panel (d).

the Au(111) again after each set of measurements. Propynyl-trioxatriangulenium (P-TOTA) molecules [16] were mixed with 40% Ethyl-TOTA [18] and deposited onto Au(111) at ambient temperature from a heated Ta crucible. Here, we exclusively report the results for P-TOTA. Submonolayer coverages were prepared to enable tip preparation on clean Au.

P-TOTA [Fig. 1(a)] was designed to ensure an upright and freestanding position of the propynyl group on a metal surface. The coupling between P-TOTA and Au is expected to be mediated by the TOTA platform and its conjugated π system. Indeed, constant current STM images of a single P-TOTA [Fig. 1(b)] reveal an upright orientation of the propynyl group. The TOTA platform appears as a low triangular protrusion ($\lesssim$1.6 Å), whereas the propynyl group is imaged as a central, circular protrusion with a maximum apparent height of $\approx$3.2 Å. Cross-sectional profiles through the protrusion reveal a shallow minimum at the center [Fig. 1(c)]. The qualitative agreement of the experimental and the theoretical cross-sectional profiles [Fig. 1(c)] indicates that the ring of maximum apparent height is caused by the topmost H atoms of the propynyl group [16].

Next, the conductance G was measured, while the tip was brought closer to the center of P-TOTA at a speed of 16.5 Å/s. The measurements were conducted on molecules in clusters to prevent lateral movements [16]. Figure 1(d) displays the measured conductance $G(\Delta z)$ of P-TOTA (blue curve) vs the tip excursion Δz towards the molecule. Zero displacement corresponds to the position of the tip before opening the feedback loop of the STM. The exponential increase of G in the tunneling region corresponds to an apparent barrier height of 4 eV, similar to that of clean Au(111) measured with a Au tip. Starting at $\approx 10^{-4}$ G_0, the slope decreases drastically indicating a mechanical contact between the tip and the molecule. Counterintuitively, the conductance decreases by a factor of $\approx$2, although the tip is moved closer to the molecule by 1 Å. At a conductance of $\approx 10^{-3}$ G_0, surprisingly, a sudden jump by almost 1 order of magnitude in the conductance occurs. This remarkable conductance variation exhibits no hysteresis and is highly reproducible. STM imaging before and after the conductance measurements revealed no change of the P-TOTA and its environment.

The transport properties of P-TOTA in a STM junction were calculated using density functional theory (DFT) combined with nonequilibrium Green's function (NEGF) methods. The supercell contained a single P-TOTA molecule adsorbed on a 10-layer Au(111) slab with 6×6 periodicity, and a Au(111) 10-atom tetrahedron mounted on the reverse side, representing the STM tip. The electronic structure and geometries were obtained with the Siesta code [19] on a $2 \times 2 \times 1$ k mesh while the elastic transmission was computed with TranSiesta [20,21] on a finer 21×21 k mesh. Dispersion interactions were taken into account by the nonlocal optB88-vdW functional [16,22].

Figure 1(d) also displays the calculated zero-bias conductance (black dots) versus electrode separation.

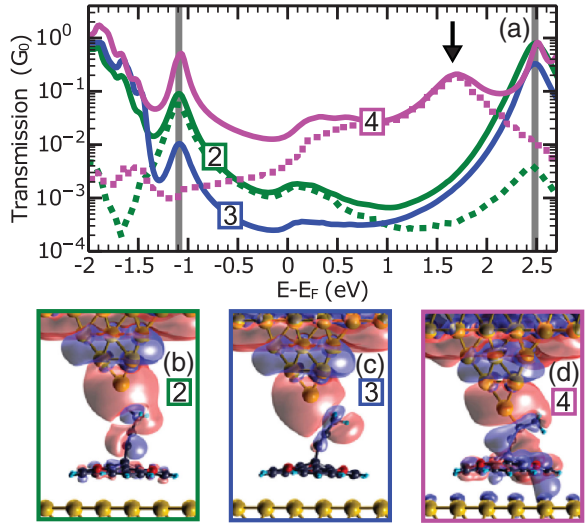

FIG. 2. (a) Calculated transmission functions vs energy for configurations **2**–**4** (solid lines). Vertical gray bars indicate resonances related to the HOMO and LUMO states of an isolated P-TOTA. For **2** and **4** the transmission functions were also calculated by projection onto MPSH eigenstates (Figs. S4 and S5 [16]), that dominate at E_F, namely, the HOMO for **2** and LUMO for 4 (dashed lines) [21]. (b)–(d) Isosurface plots of the real part of the most transmitting eigenchannel scattering states of **2**–**4** at E_F. Electron waves are incoming from the tip electrode at the $\bar{\Gamma}$ point [25–27].

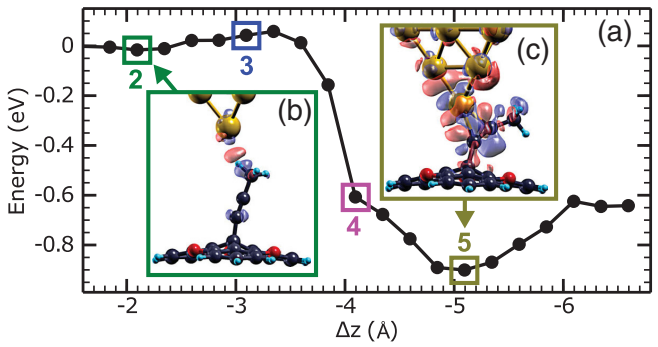

FIG. 3. (a) Energy change of the tip-molecule subsystem versus tip displacement Δz with data highlighted corresponding to configurations **2**–**5** from Fig. 1. (b)–(c) Electron density redistributions for the tip and the molecule as a result of the tip-molecule interaction before and after bond formation. Blue (red) colored isosurfaces correspond to depletion (accumulation) of electron density.

These results closely follow the experimental ones, both in the tunneling and the contact regimes. As shown in the lower panels of Fig. 1, P-TOTA is strongly distorted as the tip is approaching. For large electrode separations ($\Delta z \geq -3.5$ Å, configurations **1**–**3**), the bond angle between the propynyl moiety and the platform decreases drastically by ≈20°, whereas the corresponding deformation energy is below ≈100 meV [16]. Hence, the bond between the propynyl group and the sp^3 C atom of the TOTA platform is highly flexible [23]. The abrupt jump at conformation **4**, however, suggests a different origin.

Figure 2(a) presents transmission functions computed for electrode separations **2**–**4** in Fig. 1. At large separation (**2**) the electron transport around E_F is dominated by the nearly degenerate highest occupied molecular orbitals (HOMOs) at ≈ -1.1 eV, while the nearly degenerate lowest unoccupied molecular orbitals (LUMOs) at ≈2.3 eV are essentially unimportant. This is shown by a projection of the transmission onto the nearly degenerate HOMOs and LUMOs (Figs. S4–S6 [16]) of the molecular projected self-consistent Hamiltonian (MPSH) [16,21,24]. Accordingly, the projection onto the dominant HOMO hardly changes the transmission close to E_F [green dashed line in Fig. 2(a)].

The counterintuitive conductance reduction from **2** to **3** can be understood from the calculations as a result of a reduced coupling between the states of the tip and the molecule. As revealed by the eigenchannel scattering states [25–27], the tip s wave shifts from entering a molecular lobe at **2** [Fig. 2(b)] closer to a nodal plane of the functional group in **3** [Fig. 2(c)]. As a result the amplitude of the scattering states on the molecular TOTA platform, and consequently the transmission, is suppressed. The importance of orbital symmetry matching for the conductance has recently also been pointed out for a CO-terminated tip tunneling to a acetylene molecule in the Supplemental Material to Ref. [28].

The above transport scenario is changed as the tip moves even closer and breaks the C ≡ C triple bond as in **4** (Fig. 2). The energy spectrum of this tip-molecule structure is new and different [black arrow in Fig. 2(a)] as one of the LUMOs strongly hybridize with tip states, while the HOMOs remain largely unaffected. The projection of the transmission onto MPSH eigenstates (Fig. S6) now reveals that a broad LUMO resonance dominates transport near E_F [magenta dashed line in Fig. 2(a)]. Along with a reduced electrode separation, the tip-LUMO hybridization augments the transmission by about 2 orders of magnitude over a wide energy range. This is also reflected in the transmitting eigenchannel scattering state at E_F [Fig. 2(d)], where the delocalization over the molecular junction is evident and the bottleneck of transmission is restricted to the platform-to-substrate interface.

To understand the tip-induced chemistry in more detail we analyzed the energetics and electronic structure of the tip and molecule subsystems to single out the interplay between them without the influence of the platform-substrate interface [29]. The energy of tip and molecule varies as a function of Δz as shown in Fig. 3(a). For small separations ($\Delta z \leq -3.5$ Å), between **3** and **4**, we find a drastic energy decrease by ≈600 meV over a range of only 0.5 Å. This value mainly results from an energy gain of ≈1 eV due to increased interaction of the tip and the molecule [30] and an energy of ≈450 meV required to further deform the propynyl moiety itself [16]. Together with the small distance of 2.2 Å between the apex atom

and the molecule, this further corroborates the breaking of a C ≡ C bond and the formation of a new covalent bond to the apex Au atom as illustrated in Fig. 1. For even smaller electrode separations ($\Delta z < -3.5$ Å), we find an energy minimum in **5**. Here the tip apex atom has almost identical distances (≈2.25 Å) from two C atoms of the propynyl moiety, which were originally triple bonded (Fig. 1). Such a bonding scheme of gold clusters or cationic gold atoms to triple-bonded C atoms (Au—C—C bond) is well studied, because it represents the highly important activation step of C ≡ C triple bonds towards nucleophiles in a catalytic cycle [16,17,31,32]. Electron density is withdrawn from the bonding orbitals by the Au which makes the carbon atoms susceptible to nucleophilic attack [33].

To analyze the electron density change due to the bond formation, we define the electron density redistribution as the difference of the density of the entire junction and the densities of its two components, namely, the molecule and the tip + surface, both with frozen geometries like in the entire junction. For **2** there is only very little charge redistribution [Fig. 3(b)], which can be understood by electrostatic interaction of the tip and the molecule. By contrast, there is a large and complex charge redistribution in **5** within tip and molecule [Fig. 3(c)] due to the formation of a Au—C—C bond. Moreover, Fig. 3(c) confirms a density reduction at the originally triple bonded C atoms at the opposite side of the Au—C—C bond. A withdrawal of electrons actually is a necessary condition for the activation of a C ≡ C triple bond [33].

Remarkably, in all configurations from **4** to **5** the Au tip apex atom binds to at least one of the originally triple bonded C atoms. These novel bond configurations are mechanically constrained and all show a withdrawal of electronic charge similar to **5** [16].

Although the calculated conductance values follow closely the experimental data, they do not exhibit a jump during bond formation as observed in the experiment (Fig. 1). We attribute this difference to the elasticity of the tip shaft and a corresponding elongation of the tip during the bond formation as proposed in Refs. [34,35], which is not included in the atomistic calculations. For this reason, the experimentally observed conductance right after the sudden jump in the conductance cannot be unambiguously assigned to a specific configuration between **4** and **5**. Furthermore, G is systematically overestimated in the model which we ascribe to the tendency of DFT to underestimate HOMO-LUMO gaps [36].

Conductance data measured with different tips and molecules are remarkably similar. For most electrode separations Δz, they vary by less than a factor of ≈1.4. However, in the range $\Delta z \in [-3.5\ \text{Å}, -1.8\ \text{Å}]$ the scatter is more obvious (factor of ≈3) [16]. Our tip preparation ensures an atomically sharp tip apex. Thus, the remaining differences may be attributed to the *mesoscopic* tip shape, which affects long range dispersion and electrostatic forces. In the range between **2** and **3**, where repulsion between the apex atom and methyl moiety prevails, the long-range forces apparently exert a larger influence on the geometry than at closer distances, where a strong covalent bond is forming. These results suggest that combining an anchoring unit for covalent bonding, a C ≡ C triple bond in the present case, and a degree of flexibility within a molecule helps to achieve reproducible bonding geometries and conductances [37].

In summary, we have presented two effects that oppositely affect the conductance of P-TOTA during contact formation. At large electrode separation, the flexibility of P-TOTA causes a symmetry mismatch of the tip and molecule orbitals and reduces the conductance. At closer distances, a covalent bond between the Au tip and a C ≡ C triple bond reversibly forms under mechanical control. This bond induces new delocalized states near E_F that increase the conductance by more than 1 order of magnitude.

Moreover, the results demonstrate that TOTA is a useful platform for geometrical decoupling of a molecular subunit from a metal substrate and neighboring molecules. Interestingly, Au—C—C bonds play an important role in the activation of C ≡ C triple bonds. Thus our results hint that it may be possible to design a mechanically controlled single molecule catalyst.

We thank Lynn Gross, Carmen Herrmann, Igor Poltavskyi, and Alexandre Tkatchenko for discussions and the Deutsche Forschungsgemeinschaft (SFB 677) and the Basque Department of Education (PI-2016-1-0027) for financial support.

*jasper-toennies@physik.uni-kiel.de

[1] L. Lafferentz, F. Ample, H. Yu, S. Hecht, C. Joachim, and L. Grill, Science **323**, 1193 (2009).
[2] M. Koch, F. Ample, C. Joachim, and L. Grill, Nat. Nanotechnol. **7**, 713 (2012).
[3] G. Reecht, F. Scheurer, V. Speisser, Y. J. Dappe, F. Mathevet, and G. Schull, Phys. Rev. Lett. **112**, 047403 (2014).
[4] C. Nacci, F. Ample, D. Bleger, S. Hecht, C. Joachim, and L. Grill, Nat. Commun. **6**, 7397 (2015).
[5] C. Thiele, L. Gerhard, T. R. Eaton, D. M. Torres, M. Mayor, W. Wulfhekel, H. v Löhneysen, and M. Lukas, New J. Phys. **17**, 053043 (2015).
[6] G. Reecht, H. Bulou, F. Scheurer, V. Speisser, F. Mathevet, C. González, Y. J. Dappe, and G. Schull, J. Phys. Chem. Lett. **6**, 2987 (2015).
[7] M. C. Chong, G. Reecht, H. Bulou, A. Boeglin, F. Scheurer, F. Mathevet, and G. Schull, Phys. Rev. Lett. **116**, 036802 (2016).
[8] R. Temirov, A. Lassise, F. B. Anders, and F. S. Tautz, Nanotechnology **19**, 065401 (2008).
[9] N. Fournier, C. Wagner, C. Weiss, R. Temirov, and F. S. Tautz, Phys. Rev. B **84**, 035435 (2011).
[10] G. Reecht, C. Lotze, D. Sysoiev, T. Huhn, and K. J. Franke, ACS Nano **10**, 10555 (2016).

[11] N. J. Tao, Nat. Nanotechnol. **1**, 173 (2006).
[12] F. Schwarz and E. Lörtscher, J. Phys. Condens. Matter **26**, 474201 (2014).
[13] B. Baisch, D. Raffa, U. Jung, O. M. Magnussen, C. Nicolas, J. Lacour, J. Kubitschke, and R. Herges, J. Am. Chem. Soc. **131**, 442 (2009).
[14] N. L. Schneider, F. Matino, G. Schull, S. Gabutti, M. Mayor, and R. Berndt, Phys. Rev. B **84**, 153403 (2011).
[15] L. Gerhard, K. Edelmann, J. Homberg, M. Valášek, S. G. Bahoosh, M. Lukas, F. Pauly, M. Mayor, and W. Wulfhekel, Nat. Commun. **8**, 14672 (2017).
[16] See Supplemental Material at http://link.aps.org/supplemental/10.1103/PhysRevLett.119.066801 for details of the synthesis, the experiment, the calculations, the deformation energy, and the molecular orbitals and the MPSH states of P-TOTA; a comparison of the bond geometry of the Au tip and P-TOTA with Ref. [17], the electron charge distribution, and a comparison of conductance curves measured with different tips.
[17] G. Bistoni, P. Belanzoni, L. Belpassi, and F. Tarantelli, J. Phys. Chem. A **120**, 5239 (2016).
[18] The mixture was used to perform two experiments in parallel on the same sample.
[19] J. M. Soler, E. Artacho, J. D. Gale, A. Garía, J. Junquera, P. Ordejón, and D. Sánchez-Portal, J. Phys. Condens. Matter **14**, 2745 (2002).
[20] M. Brandbyge, J.-L. Mozos, P. Ordejón, J. Taylor, and K. Stokbro, Phys. Rev. B **65**, 165401 (2002).
[21] N. Papior, N. Lorente, T. Frederiksen, A. García, and M. Brandbyge, Comput. Phys. Commun. **212**, 8 (2017).
[22] J. Klimeš, D. R. Bowler, and A. Michaelides, J. Phys. Condens. Matter **22**, 022201 (2010).
[23] N. Hauptmann, L. Groß, K. Buchmann, K. Scheil, C. Schütt, F. L. Otte, R. Herges, C. Herrmann, and R. Berndt, New J. Phys. **17**, 013012 (2015).
[24] K. Stokbro, J. Taylor, M. Brandbyge, J.-L. Mozos, and P. Ordejon, Comput. Mater. Sci. **27**, 151 (2003).
[25] M. Paulsson and M. Brandbyge, Phys. Rev. B **76**, 115117 (2007).
[26] T. Frederiksen, M. Paulsson, M. Brandbyge, and A.-P. Jauho, Phys. Rev. B **75**, 205413 (2007).
[27] The Inelastica software suite is freely available at http://sourceforge.net/projects/inelastica.
[28] M. Corso, M. Ondráček, C. Lotze, P. Hapala, K. J. Franke, P. Jelínek, and J. I. Pascual, Phys. Rev. Lett. **115**, 136101 (2015).
[29] Technically, the substrate atoms were removed without modifying the molecule-tip atom positions. We checked that basis set superposition errors amount to less than 10% in the binding energy and thus do not qualitatively affect the reported results.
[30] For $\Delta z = -3.6$, -4.1, and -5.1 Å the interaction energies of the tip and the molecule are -0.22, -1.22, and -1.50 eV. Here, the interaction energy is defined as the energy of the entire tip-molecule subsystem minus the energies of the isolated molecule and tip, both calculated at the same geometries as in the entire tip-molecule subsystem.
[31] Y. Wang, M. Zhu, L. Kang, and B. Dai, RSC Adv. **4**, 38466 (2014).
[32] F. Ferraro, J. F. Pérez-Torres, and C. Hadad, J. Phys. Chem. C **119**, 7755 (2015).
[33] A. C. Tsipis, Organometallics **29**, 354 (2010).
[34] U. Landman, W. D. Luedtke, N. A. Burnham, and R. J. Colton, Science **248**, 454 (1990).
[35] N. Hauptmann, F. Mohn, L. Gross, G. Meyer, T. Frederiksen, and R. Berndt, New J. Phys. **14**, 073032 (2012).
[36] R. W. Godby, M. Schlüter, and L. J. Sham, Phys. Rev. Lett. **56**, 2415 (1986).
[37] Usually G critically depends on the atomic geometry. A notable exception has been reported for the amine–Au bond [38].
[38] S. Y. Quek, L. Venkataraman, H. J. Choi, S. G. Louie, M. S. Hybertsen, and J. B. Neaton, Nano Lett. **7**, 3477 (2007).

Conductance of a Freestanding Conjugated Molecular Wire
SUPPLEMENTARY ONLINE MATERIAL

Torben Jasper-Toennies,[1,*] Aran Garcia-Lekue,[2,3] Thomas Frederiksen,[2]
Sandra Ulrich,[4] Rainer Herges,[4] and Richard Berndt[1]

[1] *Institut für Experimentelle und Angewandte Physik, Christian-Albrechts-Universität zu Kiel, 24098 Kiel, Germany*
[2] *Donostia International Physics Center, DIPC, Paseo Manuel de Lardizabal 4, E-20018 Donostia-San Sebastián, Spain*
[3] *IKERBASQUE, Basque Foundation for Science, E-48013 Bilbao, Spain*
[4] *Otto-Diels-Institut für Organische Chemie, Christian-Albrechts-Universität zu Kiel, 24098 Kiel, Germany*

(Dated: July 11, 2017)

SYNTHESIS OF 12C-PROPYNYL-4,8,12-TRIOXATRIANGULENE (P-TOTA)

4,8,12-trioxatriangulenium tetrafluorborate (150 mg, 403 μmol) suspended in 200 ml anhydrous tetrahydrofuran (THF) was mixed with propynyl magnesium bromide (20 mL, 10 mmol, 0.5 M in THF) under nitrogen. The reaction mixture was heated under reflux for 7 h and the solvent was removed under reduced pressure. The residue was purified by chromatography over Florisil (cyclohexane/diethyl ether 1:1). The product was obtained as a colorless solid (31.2 mg, 96.2 μmol) [1].

CONDUCTANCE MEASUREMENTS OF P-TOTA

The conductance of P-TOTA was measured on molecules in clusters, where P-TOTA is adjacent to one or two Ethyl-TOTA molecules (Fig. S1(a)) [2]. This was sufficient to prevent rotational and lateral movements of P-TOTA during the contact formation. Conductances measured with different tips and from different molecules along with calculated results are displayed in Fig. S1(b). The experimental and theoretical conductances are remarkably similar. However, there are also differences which are discussed in the manuscript.

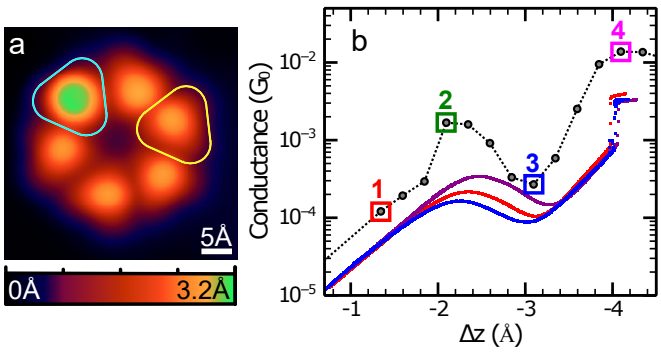

FIG. S1. (a) Constant-current STM topograph of a cluster comprising of one P-TOTA and five Ethyl-TOTA molecules (100 mV, 30 pA). A single P-TOTA (Ethyl-TOTA) is marked by a cyan (yellow) border. (b) Experimental conductance curves G(Δz) of P-TOTA measured with different tips and calculated conductance. Zero tip displacement Δz is defined by feedback loop parameters of 19 pA and 100 mV in the experiment. In the calculation, this corresponds to a distance z = 11.8 Å between the tip apex atom and the Au surface layer. Configurations **1** – **4** are indicated.

COMPUTATIONAL METHODS

SIESTA calculations [3] were done using a basis set consisting of split-valence double-zeta plus polarization DZP orbitals with 0.02 eV energy shift for the C, H and O atoms, as well as for the Au tip atoms and the surface Au atoms below the tip and the molecule. For bulk Au atoms, single-zeta plus polarization SZP orbitals with 0.02 Ry energy shift were used. Atomic coordinates of the molecule, tip, and surface gold atoms were relaxed until forces were smaller than 0.04 eV/Å. A cutoff of 400 Ry was used for the real-space grid integrations. During geometry optimization and for the TRANSIESTA calculations [4, 5] a Monkhorst-Pack mesh with $2 \times 2 \times 1$ k-point sampling of the three-dimensional Brillouin zone was used. The transmission functions were sampled over 21×21 k points. To obtain the theoretical apparent height profile for P-TOTA on Au(111) a constant current image was simulated within the Tersoff-Hamann approximation at 100 meV. Eigenchannel scattering states were computed with INELASTICA [6–8].

Deformation energy of P-TOTA

P-TOTA is strongly distorted as the tip is approaching. The corresponding deformation energies of P-TOTA in the gas phase (Fig. S2) reveal a high flexibility of the bond angle between the propynyl group and TOTA (configurations **1** – **3**). Furthermore, the more complex deformation of P-TOTA from configuration **3** to **4** significantly increases the energy. This deformation is caused by the Au–C–C bond formation between the tip and the molecule.

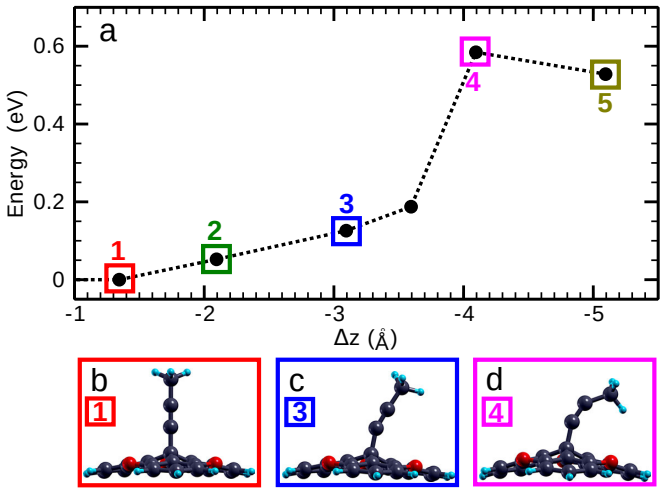

FIG. S2. (a) Deformation energy of isolated P-TOTA for various tip displacements Δz and corresponding geometries. Configurations **1** – **5** are indicated. (b)–(d) Geometry of P-TOTA in configurations **1**, **3**, and **4**.

Molecular orbitals and MPSH states

The degenerate HOMOs and nearly degenerate LUMOs of isolated P-TOTA are shown in Fig. S3. The upper and lower panels correspond to the pristine configuration **1** and the tilted configuration **3**. Figure S3 shows that these orbitals are hardly affected by the tilting of the molecule. With respect to the conductance, the most important difference between the intermediate configuration **2** and **3** is a change of the local symmetry match between the tip and molecule orbitals as described in the manuscript.

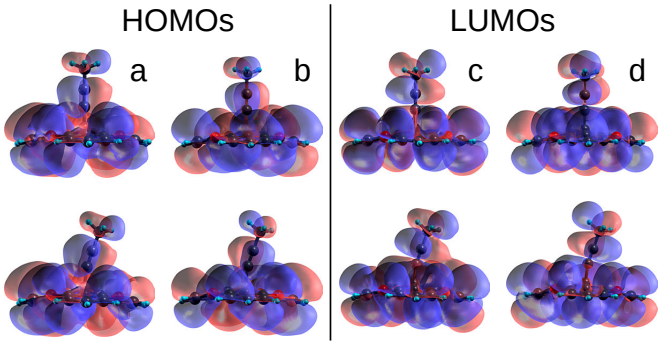

FIG. S3. Molecular orbitals of isolated P-TOTA in its undistorted form (upper row) and tilted as in **3** (lower row). (a)–(b) degenerate HOMOs, (c)–(d) nearly degenerate LUMOs. The HOMO-LUMO gap is in both configurations 3.6 eV.

To disentangle the roles of the different P-TOTA molecular states for electron transport across the junction we have performed an analysis based on the molecular projected self-consistent Hamiltonian (MPSH) [5, 9] corresponding to the subspace of P-TOTA [10]. We

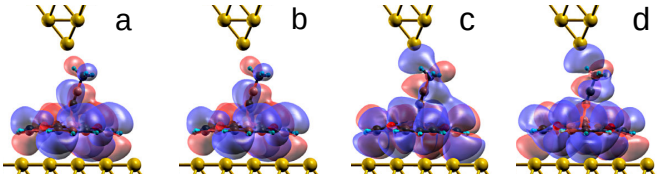

FIG. S4. HOMO-1, HOMO, LUMO, and LUMO+1 of the MPSH Hamiltonian for configuration **2** with eigenenergies $E-E_F = -1.22$, -1.17, 2.35, and 2.38 eV (left to right) used for the transmission projections presented in Fig. 2(a) and Fig. S6.

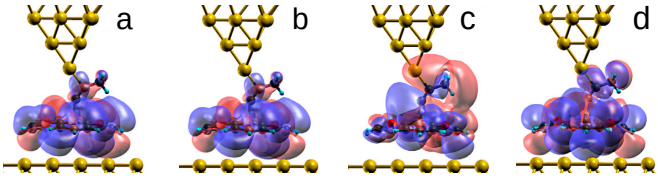

FIG. S5. HOMO-1, HOMO, LUMO, and LUMO+1 of the MPSH Hamiltonian for configuration **4** with eigenenergies $E-E_F = -1.19$, -1.14, 1.18, and 2.41 eV (left to right) used for the transmission projections presented in Fig. 2(a) and Fig. S6.

have computed the electron transmission projected onto HOMO-1, HOMO, LUMO, and LUMO+1 for the configurations **2** and **4** (states shown in Figs. S4 and S5) following the scheme presented in [5].

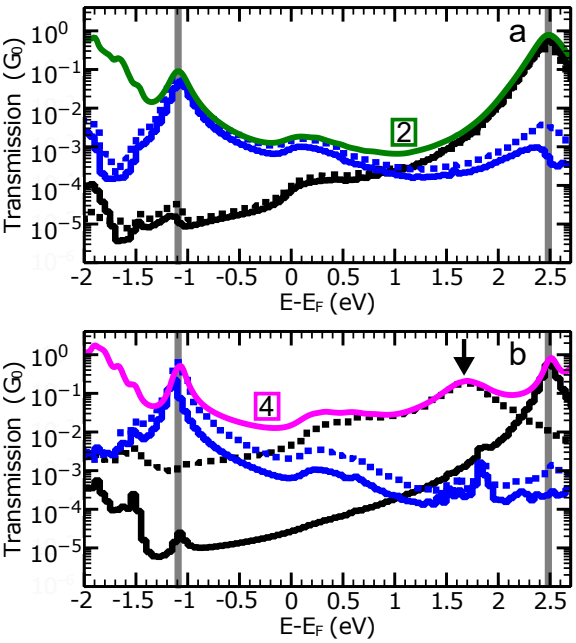

FIG. S6. Electron transmission projected onto HOMO-1 (blue solid), HOMO (blue dashed), LUMO (black dashed), and LUMO+1 (black solid line) of the MPSH Hamiltonian (Figs. S4 and S5) for the configurations **2** (a) and **4** (b) along with the full transmissions (green and magenta solid lines).

As observed in Fig. S6, for configuration **2** the transmission near E_F is dominated by the HOMO states, while for configuration **4** it changes to the strongly hybridized LUMO state (black arrow).

Au–C–C bond geometry and charge redistribution

Below, we compare our calculated Au–C–C bond geometry of configuration **5** with recent results for an ethyne molecule on a cluster of 18 Au atoms (Table S1). Both geometries are remarkably similar confirming that the mechanical approach of the Au apex atom leads to the formation of a Au−C−C bond.

Remarkably, for all configurations from **4** to **5** and smaller electrode separations the Au tip apex atom binds to at least one of the originally triple bonded C atoms. For example in **4** ($\Delta z = -4.1$ Å) the Au tip apex atom binds mainly to the carbon atom labeled C2 in Fig. S7(a). These novel bond configurations are mechanically constrained. They all show a withdrawal of electronic charge similar to the minimum energy bond geometry **5** (Fig. S8). Interestingly, the electron density redistribution due to the Au–C–C bond hardly involves the TOTA platform. Consequently, the Au substrate has negligible effect on the charge redistribution of the propynyl moiety.

TABLE S1. Calculated Au–C–C bond geometry of configuration **5** vs. calculated bond geometry of an ethyne molecule on a Au cluster [11]. d(Au,X) is the distance between the Au apex atom and atom X and ∠(X,Y,Z) the bond angle between atom X, Y and Z. The atom labels are defined in Fig. S7.

P-TOTA and Au-tip		Ethyne and Au_{18} cluster [11]	
d(Au,C1)	2.28 Å	d(Au,C1)	2.32 Å
d(Au,C2)	2.20 Å	d(Au,C2)	2.32 Å
∠(Au,C1,C2)	69.9°	∠(Au,C1,C2)	74.6°
∠(Au,C2,C1)	77.2°	∠(Au,C2,C1)	74.6°
∠(Au,C2,C3)	121.6°	∠(Au,C2,H3)	118.5°
∠(C1,C2,C3)	161.1°	∠(C1,C2,C3)	166.9°

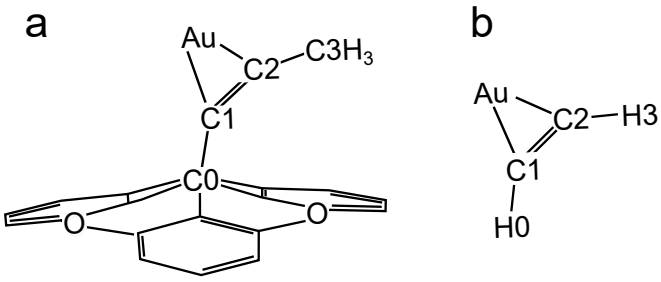

FIG. S7. Labels of the atoms involved in the Au–C–C bond between (a) the Au apex atom of the STM tip and P-TOTA or (b) the apex atom of a Au cluster and an ethyne molecule.

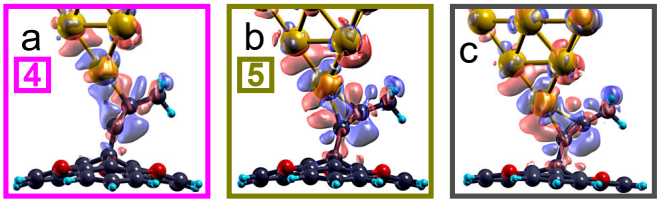

FIG. S8. (a)–(c) Electron density redistributions of the tip and the molecule caused by the tip-molecule interaction. Configurations are shown for $\Delta z = -4.1, -5.1$ and -6.1 Å. Blue (red) isosurfaces indicate depletion (accumulation) of electron density.

* jasper-toennies@physik.uni-kiel.de

[1] The compound was identified by the following nuclear magnetic resonance (NMR) and mass spetra (MS) signatures: 1H NMR (500 MHz, THF−d8): $\delta = 7.29$ (t, J=8.2 Hz, 3H, H−5), 6.97 (d, J=8.2 Hz, 6H, H−4), 1.59 (s, 3H, H−8) ppm.
13C NMR (125.8 MHz, THF−d8): $\delta =$ 153.03 (q, C−3), 129.56 (t, C−5), 112.18 (t, C−4), 111.78 (q, C−2), 81.62 (q, C−6), 80.86 (t, C−7), 22.23 (q, C−1), 3.05 (p, C−8) ppm.
MS (EI): m/z (%) = 324 (31), 285 (100).
MS (CI): m/z (%) = 325 (100), 285 (81).

[2] A mixture of P-TOTA and Ethyl-TOTA molecules was evaporated onto the Au(111) surface to acquire comparable data with the same tips. Here, we focus on P-TOTA.

[3] J. M. Soler, E. Artacho, J. D. Gale, A. García, J. Junquera, P. Ordejón, and D. Sánchez-Portal, J. Phys. Condens. Matter **14**, 2745 (2002).

[4] M. Brandbyge, J.-L. Mozos, P. Ordejón, J. Taylor, and K. Stokbro, Phys. Rev. B **65**, 165401 (2002).

[5] N. Papior, N. Lorente, T. Frederiksen, A. García, and M. Brandbyge, Comp. Phys. Comm. **212**, 8 (2017).

[6] M. Paulsson and M. Brandbyge, Phys. Rev. B **76**, 115117 (2007).

[7] T. Frederiksen, M. Paulsson, M. Brandbyge, and A.-P. Jauho, Phys. Rev. B **75**, 205413 (2007).

[8] The Inelastica software suite is freely available at `http://sourceforge.net/projects/inelastica`.

[9] K. Stokbro, J. Taylor, M. Brandbyge, J.-L. Mozos, and P. Ordejon, Comput. Mater. Sci. **27**, 151 (2003).

[10] For configuration **4**, where the electrode distance is quite short, we had to reduce the extension of the basis orbitals on the Au apex atom to allow folding of the electrode self-energies fully on the molecular part. In practice, we used the same, more short-ranged SZP basis as used for the bulk Au atoms.

[11] G. Bistoni, P. Belanzoni, L. Belpassi, and F. Tarantelli, J. Phys. Chem. A **120**, 5239 (2016).